

Metallic and Non-superconducting Phases in $LnBa_2Cu_{3-x}Ni_xO_{7+\delta}$ Oxides¹

S. Sundar Manoharan, S. Ramesh, M. S. Hegde, and G. N. Subbanna*

*Solid State and Structural Chemistry Unit, *Materials Research Centre, Indian Institute of Science, Bangalore 560 012, India,*

Received June 1, 1993; in revised form December 7, 1993; accepted December 10, 1993

A series of compounds $LaBa_2Cu_{3-x}Ni_xO_{7\pm\delta}$ ($0.0 < x < 0.3$) and $LnBa_2Cu_{3-x}Ni_xO_{7-\delta}$ ($Ln123$; $Ln = Pr, Nd, Sm, Gd, \text{ and } Er$; $x = 0.1, 0.2$) has been synthesized by a ceramic method and their structure characterized by X-ray and electron diffraction. The substitution of nickel in $LaBa_2Cu_3O_{7\pm\delta}$ ($La123$) induces an orthorhombic to tetragonal structural transition as well reducing the activation energy for oxygen desorption. Orthorhombicity increased with decreasing lanthanide ion radius in the $LnBa_2Cu_{2.9}Ni_{0.1}O_{7\pm\delta}$ system. Electrical resistivity measurements show metallic behavior down to 4.2 K for $LaBa_2Cu_{3-x}Ni_xO_{7\pm\delta}$ ($0.1 < x < 0.3$). The superconducting transition temperatures of Ni-doped $Ln123$ decreased with increasing rare earth ion radius, for the same nickel content. These properties are discussed in terms of the Ni^{3+} ion occupying the Cu(1) sites in $La123$ stabilized by a larger La^{3+} ion and Ni^{2+} ion occupying the Cu(2) sites in the $Ln123$ system of oxides. © 1994 Academic Press, Inc.

1. INTRODUCTION

An extensive literature exists on the substitution of transition metals for copper in the superconducting $YBa_2Cu_3O_{7-\delta}$ ($Y123$) system (1–6). *Huang et al.* (7) have classified the transition metal substitution for Cu in the $Y123$ system into three categories: (a) those with only partial replacement of Cu(1) and/or Cu(2) sites; (b) those in which Cu(1) is replaced completely; and (c) those in which all three Cu are replaced by other metal ions. All such studies were aimed at understanding the mechanism responsible for superconductivity and the structural chemistry of the $Y123$ system. The substitution of transition metal ions for copper gained importance due to the fact that the replacement of yttrium by rare earths with larger magnetic moments has a relatively smaller effect on the superconducting transition temperature or other physical properties. This observation has led to the general idea that the metallic and superconducting properties

of these materials are governed mainly by the Cu-3d and O-2p band overlap (8). One of the interesting problems encountered with the transition metal substitution was to precisely assign the position of the substituted metal ion either at the chain Cu(1) site or at the sheets Cu(2) sites. This becomes important as the position of the transition metal ion can bring about dramatic changes in the structure and physical properties of the system. Neutron Rietveld refinement, anomalous X-ray scattering studies, and a single-crystal X-ray study have shown that Fe, Co, and Al are known to partially substitute the Cu(1) site, whereas Zn and Ni prefer to occupy the Cu(2) sites in $Y123$ (9–11). The above site preferences for these particular ions in the $Y123$ system are almost independent of the method of preparation, for example, postannealing. However, the effect of various rare earth ions on the site preferences of these cations and hence on the structural and related properties of the system has not been investigated thoroughly. For example, iron has been shown to preferentially occupy the Cu(2) sites in $LaBa_2Cu_3O_{7\pm\delta}$ ($La123$) (12) versus the Cu(1) site preferred in $Y123$.

We have recently investigated the cobalt substitution in $LnBa_2Cu_3O_{7+\delta}$ ($Ln = La, Pr$) and have shown by X-ray diffraction, electron microscopy, and chemical reactivity studies that cobalt prefers to occupy the Cu(2) sites (13, 14). Lanthanum, owing to its larger ionic size, lesser acidity, and smaller electronegativity compared to other rare earth ions, exhibits different chemistry in these oxides. In an attempt to elucidate further the structural trends and physical properties in these materials we have investigated the substitutional effects of Ni for Cu in $LnBa_2Cu_3O_{7+\delta}$ ($Ln = La, Pr, Nd, Sm, Gd, Y, \text{ and } Er$) system of oxides. In the present paper we present the structural chemistry, oxygen mobility, and electrical properties in the $LnBa_2Cu_{3-x}Ni_xO_{7\pm\delta}$ ($0 < x < 0.2$) system of oxides. When Ni was substituted for Cu in $YBa_2Cu_3O_{7-\delta}$, the oxide was metallic and superconducting (2). We find that Ni in $LaBa_2Cu_{3-x}Ni_xO_{7+\delta}$ for $0.1 < x < 0.3$ is non-superconducting but metallic, which is unique among the cation-substituted $Y123$ system of oxides.

¹ Contribution No. 1001 from the Solid State and Structural Chemistry Unit.

2. EXPERIMENTAL

The samples $\text{LaBa}_2\text{Cu}_{3-x}\text{Ni}_x\text{O}_{7\pm\delta}$ ($0 < x < 0.3$), $\text{LnBa}_2\text{Cu}_{2.9}\text{Ni}_{0.1}\text{O}_{7\pm\delta}$ ($\text{Ln} = \text{Pr, Nd, Sm, Gd, and Er}$), and $\text{LnBa}_2\text{Cu}_{2.8}\text{Ni}_{0.2}\text{O}_{7-\delta}$ ($\text{Ln} = \text{Nd, Sm, and Y}$) were prepared by a ceramic method. The synthesis was carried out by grinding stoichiometric amounts of component oxides Ln_2O_3 (Pr_6O_{11}), CuO , BaO_2 , and $\text{Ni}(\text{C}_2\text{O}_4) \cdot 2\text{H}_2\text{O}$ (chemically analyzed) and heating them at 950°C for 48 hr with three intermittent grindings. The calcined powders were compacted into $3 \times 10\text{-mm}$ discs and sintered at 950°C for 10 hr. The sintered samples were cooled from 700 to 350°C in a stream of oxygen at the rate of $1^\circ\text{C}/\text{min}$ and then annealed at 350°C for 24 hr prior to further cooling to room temperature.

The polycrystalline materials were examined for phase purity and cell parameters by the X-ray diffraction technique employing a JEOL-JDX 8P powder diffractometer with $\text{CuK}\alpha$ radiation. The oxygen content in the samples was analyzed by an iodometric titration method (15). The structure of the typical $\text{LaBa}_2\text{Cu}_{2.9}\text{Ni}_{0.1}\text{O}_{7\pm\delta}$ oxide was also examined by an electron microscopic technique using a JEOL 200 CX transmission electron microscope.

Oxygen desorption experiments were carried out employing a homebuilt desorption apparatus (16). A typical desorption run was carried out by heating 250 mg of the powder sample in an evacuated silica reactor at a rate of $15^\circ\text{C}/\text{min}$ at 10^{-5} Torr vacuum. The emanating oxygen gas was monitored by an on-line quadrupole mass spectrometer. Electrical resistivity measurements as a function of temperature were carried out on the well-sintered and oxygen-annealed pellets by the standard four-probe method down to 15 K. The $\text{LaBa}_2\text{Cu}_{3-x}\text{Ni}_x\text{O}_{7\pm\delta}$ samples were also tested for superconductivity down to 4.2 K by a nonresonant microwave absorption technique (17) employing a Bruker ESR spectrometer ER-300D, equipped with an Oxford helium flow cryostat.

3. RESULTS

3.1. X-Ray Diffraction

Single-phase solid solutions of $\text{LaBa}_2\text{Cu}_{3-x}\text{Ni}_x\text{O}_{7\pm\delta}$ were obtained in the concentration range $0 < x < 0.3$. Figure 1 shows the X-ray diffractograms of the $\text{LaBa}_2\text{Cu}_{3-x}\text{Ni}_x\text{O}_{7\pm\delta}$ ($0.0 < x < 0.3$). The orthorhombicity of the parent La123 is evident from the splitting of (020) and (200) reflections. Nickel-substituted samples showed no such splitting (curves b to e), unlike $\text{YBa}_2\text{Cu}_{2.9}\text{Ni}_{0.1}\text{O}_{7-\delta}$ (curve f) shown in the figure for comparison. The synthesis of single-phase $\text{LaBa}_2\text{Cu}_3\text{O}_7$ with a superconducting transition temperature (T_c) of 90 K has been found to be difficult by the normal ceramic method. High-quality phases of La123 have been made by sintering in N_2 atmo-

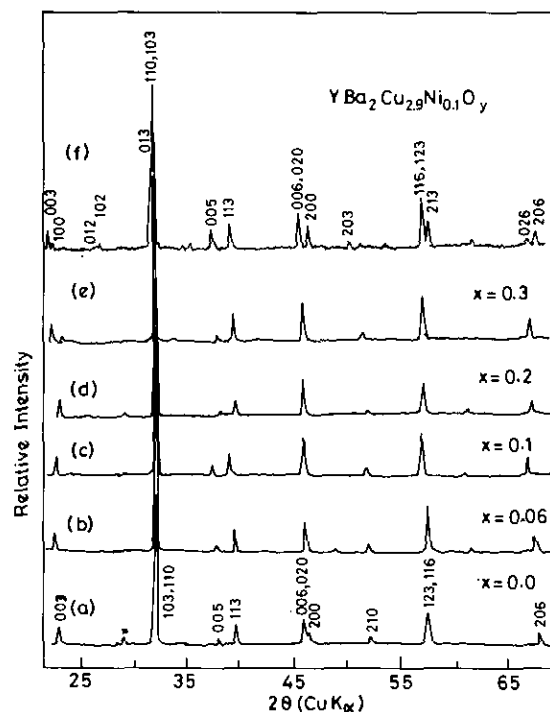


FIG. 1. X-ray diffractograms of (a) $\text{LaBa}_2\text{Cu}_3\text{O}_{7\pm\delta}$, (b) $\text{LaBa}_2\text{Cu}_{2.94}\text{Ni}_{0.06}\text{O}_{7\pm\delta}$, (c) $\text{LaBa}_2\text{Cu}_{2.9}\text{Ni}_{0.1}\text{O}_{7\pm\delta}$, (d) $\text{LaBa}_2\text{Cu}_{2.8}\text{Ni}_{0.2}\text{O}_{7\pm\delta}$, (e) $\text{LaBa}_2\text{Cu}_{2.7}\text{Ni}_{0.3}\text{O}_{7-\delta}$, and (f) $\text{YBa}_2\text{Cu}_{2.9}\text{Ni}_{0.1}\text{O}_{7\pm\delta}$ for comparison.

sphere and postannealing under flowing oxygen at 300°C (18, 19). The parent La123 prepared in the present study contained a small amount ($\approx 3\%$) of BaCuO_2 impurity. However, the Ni-doped samples were obtained without any BaCuO_2 impurity up to a composition of $x = 0.3$. Higher compositions of nickel ($x > 0.3$), however, started yielding multiphase materials. The lattice parameters and oxygen contents of these oxides are summarized in Table 1. There was a gradual increase in the oxygen content with an increase in Ni content, and it exceeded 7 in the case of Ni-doped samples. The variation of the a , b , and $c/3$ parameters for the $\text{LaBa}_2\text{Cu}_{3-x}\text{Ni}_x\text{O}_{7\pm\delta}$ system is shown in Fig. 2. The transition from orthorhombic to tetragonal symmetry occurred with a relatively lower content of Ni ($x = 0.06$).

$\text{CuK}\alpha$ x-ray diffraction patterns of the $\text{LnBa}_2\text{Cu}_{2.9}\text{Ni}_{0.1}\text{O}_{7-\delta}$ ($\text{Ln} = \text{La, Pr, Nd, Sm, Gd, and Er}$) samples are shown in Fig. 3. The tetragonal to orthorhombic transition is clearly evident as the cationic radii decrease. $\text{LnBa}_2\text{Cu}_{2.8}\text{Ni}_{0.2}\text{O}_{7-\delta}$ ($\text{Ln} = \text{Nd, Sm, and Y}$) were also synthesized without any impurity phase. The a , b , and c parameters, cell volume, and oxygen content are listed in Table 2. It is important to note that the oxygen content is less than 7 in all these oxides except in Ni-doped La123. Figure 4 gives the variation of a , b , and $c/3$ as a function of the rare earth radius. All the unit cell parameters decrease with decreasing rare earth ion radius. Among this series,

TABLE 1
Lattice Parameters^a and Oxygen^b Contents of the $\text{LaBa}_2\text{Cu}_{3-x}\text{Ni}_x\text{O}_{7+\delta}$ System

System	Structure	Lattice constants (Å)			Cell volume (Å ³)	Oxygen content
		<i>a</i>	<i>b</i>	<i>c</i>		
$\text{LaBa}_2\text{Cu}_3\text{O}_{7\pm\delta}$	O	3.902	3.918	11.754	179.42	6.99
$\text{LaBa}_2\text{Cu}_{2.94}\text{Ni}_{0.06}\text{O}_{7\pm\delta}$	T	3.919	3.919	11.744	180.37	7.03
$\text{LaBa}_2\text{Cu}_{2.9}\text{Ni}_{0.1}\text{O}_{7\pm\delta}$	T	3.917	3.917	11.752	180.30	7.05
$\text{LaBa}_2\text{Cu}_{2.8}\text{Ni}_{0.2}\text{O}_{7\pm\delta}$	T	3.912	3.912	11.740	179.66	7.12
$\text{LaBa}_2\text{Cu}_{2.7}\text{Ni}_{0.3}\text{O}_{7\pm\delta}$	T	3.913	3.913	11.744	179.82	7.15

Note. O, orthorhombic; T, tetragonal.

^a Accurate within ± 0.004 .

^b Accurate within ± 0.03 .

only the lanthanum compound obeys the relation $a = b = c/3$. The degree of orthorhombicity defined as $(b - a)/(b + a)$ increased systematically with decreasing lanthanide ion radius as shown in the inset of Fig. 4. A similar behavior has been observed when yttrium ion is replaced by different rare earths in Y123 (20).

3.2. Electron Microscopy

The parent La123 sample showed a twinned microstructure characteristic of the orthorhombic structure in the

123 system (21). The selected area diffraction patterns for the $\text{LaBa}_2\text{Cu}_{2.9}\text{Ni}_{0.1}\text{O}_{7+\delta}$ are given in Fig. 5. The diffraction pattern along the $[0\ 0\ 1]$ zone axis shown in Fig. 5a with the relation $a^* = b^*$ is indicative of the tetragonal structure of the sample. The diffraction pattern for the same composition along the $[0\ 1\ 0]$ zone axis is shown in Fig. 5b. The relations $3c^* = a^*$ exhibited by this pattern confirms the layered triple perovskite structure. Figure 5c shows the high-resolution lattice image indicative of the 11.7-Å periodicity. Thus, the electron microscopic results confirm the tetragonal structure of $\text{LaBa}_2\text{Cu}_{2.9}\text{Ni}_{0.1}\text{O}_{7+\delta}$.

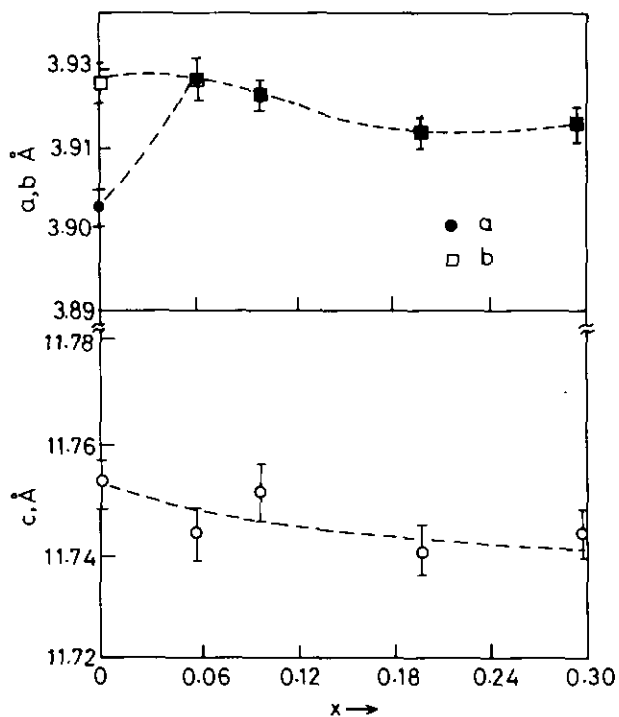


FIG. 2. Variation of the *a*, *b*, and *c* parameters as a function of nickel content *x* in the $\text{LaBa}_2\text{Cu}_{3-x}\text{Ni}_x\text{O}_{7\pm\delta}$ system.

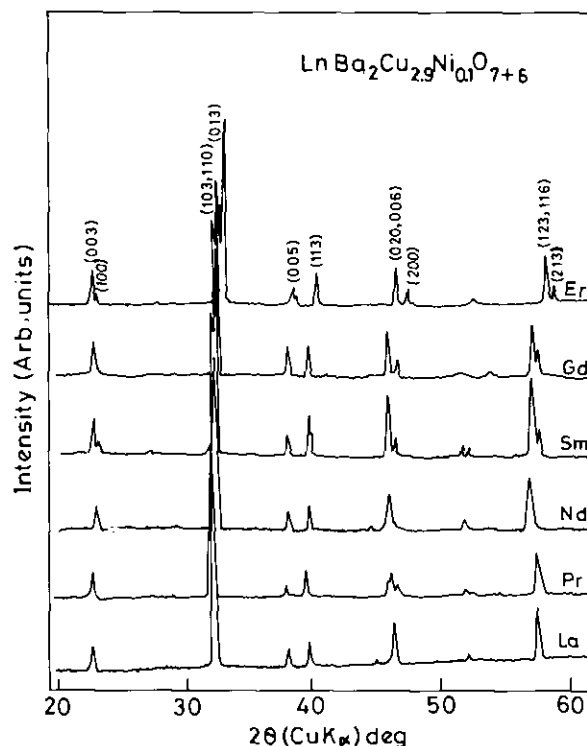


FIG. 3. X-ray diffractograms of the $\text{LnBa}_2\text{Cu}_{2.9}\text{Ni}_{0.1}\text{O}_{7\pm\delta}$ system of oxides (*Ln* = La, Pr, Nd, Sm, Gd, and Er).

TABLE 2
Cell Parameters^a and Oxygen Content^b of Oxygen-Annealed $\text{LnBa}_2\text{Cu}_{2.9}\text{Ni}_{0.1}\text{O}_{7+\delta}$

System	Lattice constants (Å)			Cell volume (Å ³)	Oxygen content	T_c (K)
	<i>a</i>	<i>b</i>	<i>c</i>			
$\text{LaBa}_2\text{Cu}_{2.9}\text{Ni}_{0.1}\text{O}_{7\pm\delta}$	3.917	3.917	11.752	178.47	7.05	Metal
$\text{PrBa}_2\text{Cu}_{2.9}\text{Ni}_{0.1}\text{O}_{7\pm\delta}$	3.895	3.912	11.778	179.46	6.75	Semif ^c
$\text{NdBa}_2\text{Cu}_{2.9}\text{Ni}_{0.1}\text{O}_{7\pm\delta}$	3.896	3.896	11.698	177.59	6.72	55
$\text{SmBa}_2\text{Cu}_{2.9}\text{Ni}_{0.1}\text{O}_{7\pm\delta}$	3.842	3.903	11.704	175.50	6.77	65
$\text{GdBa}_2\text{Cu}_{2.9}\text{Ni}_{0.1}\text{O}_{7\pm\delta}$	3.854	3.895	11.698	175.62	6.75	71
$\text{ErBa}_2\text{Cu}_{2.9}\text{Ni}_{0.1}\text{O}_{7\pm\delta}$	3.823	3.885	11.663	173.22	6.78	71
$\text{LaBa}_2\text{Cu}_{2.8}\text{Ni}_{0.2}\text{O}_{7\pm\delta}$	3.912	3.912	11.740	179.66	7.12	Metal
$\text{NdBa}_2\text{Cu}_{2.8}\text{Ni}_{0.2}\text{O}_{7\pm\delta}$	3.908	3.908	11.721	179.10	6.93	20
$\text{SmBa}_2\text{Cu}_{2.8}\text{Ni}_{0.2}\text{O}_{7\pm\delta}$	3.836	3.890	11.624	173.45	6.89	35

^a Accurate within ± 0.004 .

^b Accurate within ± 0.03 .

^c Semiconducting.

3.3. Thermal Desorption Studies

The oxygen desorption thermograms for the series $\text{LaBa}_2\text{Cu}_{3-x}\text{Ni}_x\text{O}_{7\pm\delta}$ are given in Fig. 6. The activation energies (E_a) for oxygen desorption were obtained from the Arrhenius plots ($\ln(I)$ vs $1/T$). The inset of Fig. 6 shows the variation of E_a as a function of nickel content x . The activation energy as well as the peak temperature for

oxygen desorption decreased with increase in nickel content.

3.4. Electrical Conductivity

The variation of the resistance of the samples $\text{LaBa}_2\text{Cu}_{3-x}\text{Ni}_x\text{O}_{7\pm\delta}$ is shown in Fig. 7. The inset shows the variation of the room temperature resistivity of the samples as a function of nickel content. The sample with Ni content $x = 0.06$ shows a T_c of 18 K, whereas $x = 0.1, 0.2, 0.3$ members are all metallic down to 13 K. Nonresonance microwave absorption studies confirmed the absence of superconductivity in the samples with $x = 0.1, 0.2, 0.3$, down to 4.3 K. The room temperature resistivity of the samples increased with increasing nickel content. The temperature variation of resistance of the $\text{LaBa}_2\text{Cu}_{2.9}\text{Ni}_{0.1}\text{O}_{7-\delta}$ system of oxides is given in Fig. 8. But for $\text{LaBa}_2\text{Cu}_{2.9}\text{Ni}_{0.1}\text{O}_{7+\delta}$ and $\text{PrBa}_2\text{Cu}_{2.9}\text{Ni}_{0.1}\text{O}_{7-\delta}$, which are metallic and semiconducting, respectively, all the compounds showed a superconducting transition temperature. The rare earth ion exhibits a marked influence on the superconducting transition temperature; as the ionic radius increased, T_c decreased for the same Ni ($x = 0.1$) concentration. The inset of Fig. 8 shows the variation of T_c of this series of compounds as a function of radius of the lanthanide ion. Superconducting transition temperatures of $\text{LnBa}_2\text{Cu}_{2.8}\text{Ni}_{0.2}\text{O}_{7-\delta}$ ($\text{Ln} = \text{Nd}, \text{Sm}, \text{and Y}$) indeed confirmed such a trend, as can be seen from Table 2.

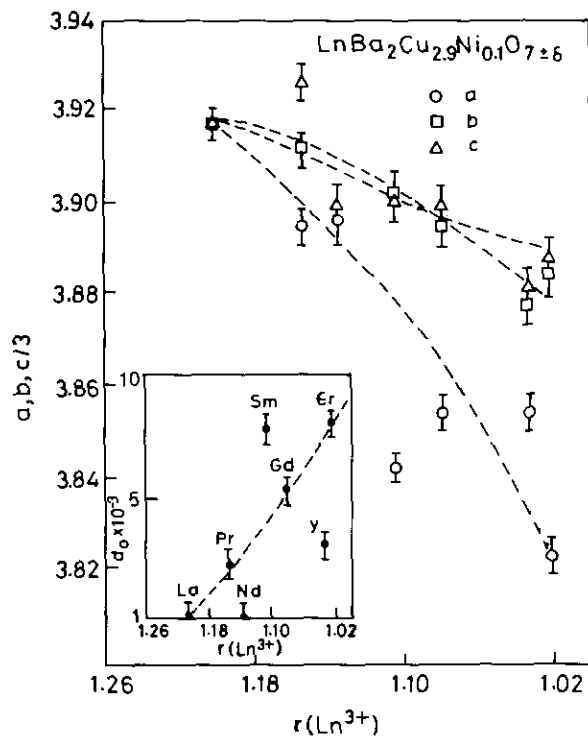


FIG. 4. The variation of lattice parameters a , b , and $c/3$ as a function of decreasing rare earth ion radius in the $\text{LnBa}_2\text{Cu}_{2.9}\text{Ni}_{0.1}\text{O}_{7\pm\delta}$ system of oxides. Inset shows the degree of orthorhombicity as a function of lanthanide ion radius.

4. DISCUSSION

The orthorhombic to tetragonal structural transition in Y123 can be induced by two effects: (a) the occupancy of oxygen ions at the normally vacant O(5) ($\frac{1}{2} 0 0$) sites, which can be achieved by substitution of a transition metal ion preferring an octahedral coordination in the place of

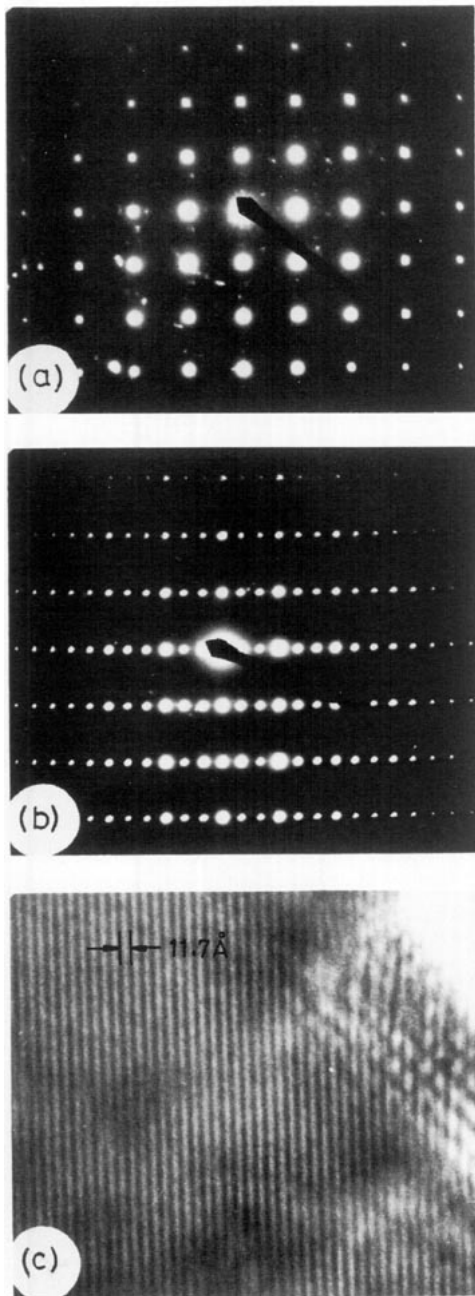


FIG. 5. Selected area diffraction patterns for tetragonal $\text{LaBa}_2\text{Cu}_{2.9}\text{Ni}_{0.1}\text{O}_{7\pm\delta}$ along the (a) $[0\ 0\ 1]$ zone axis and (b) $[0\ 1\ 0]$ zone axis. (c) High-resolution lattice image showing the 11.7-Å periodicity.

Cu(1), otherwise stabilized in a square planar configuration. Such substitutional effects causing an orthorhombic to tetragonal structural transition are generally observed with the substitution of cobalt, iron, and aluminium in Y123 (9–11). (b) Systematic removal of oxygen from the $b/2$ ($0\ \frac{1}{2}\ 0$) site associated with a plateau in the variation of transition temperature against the oxygen deficiency. This phenomenon has been extensively studied and is

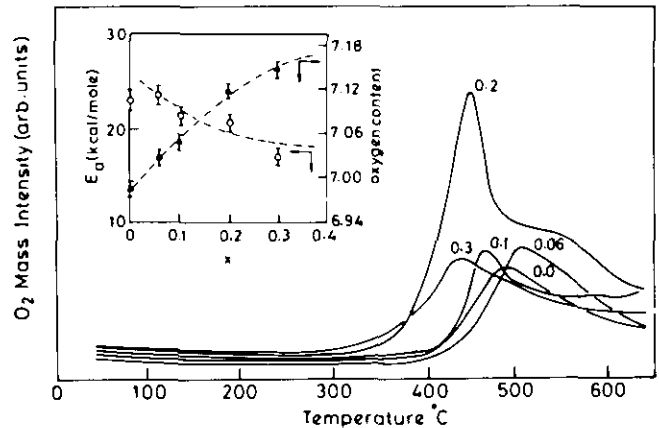


FIG. 6. Oxygen desorption thermograms for the $\text{LaBa}_2\text{Cu}_{3-x}\text{Ni}_x\text{O}_{7\pm\delta}$ system of oxides. Inset shows the variation of oxygen content and activation energy for oxygen desorption (E_a) as a function of nickel content x .

well understood (22). Going by the above arguments, if the O–T structural transition is effected by the former method, gradual substitution of a trivalent metal ion at the Cu(1) site will lead to a corresponding increase in the total oxygen content. This has been observed in the present study in the Ni-substituted La123 as can be seen in Table 1. Contrary to this, the oxygen content did not exceed 7.00 in the case of nickel-substituted $\text{LaBa}_2\text{Cu}_{3-x}\text{Ni}_x\text{O}_{7-\delta}$ ($\text{Ln} = \text{Nd}, \text{Sm}, \text{Gd}, \text{and Er}; x = 0.1, 0.2$).

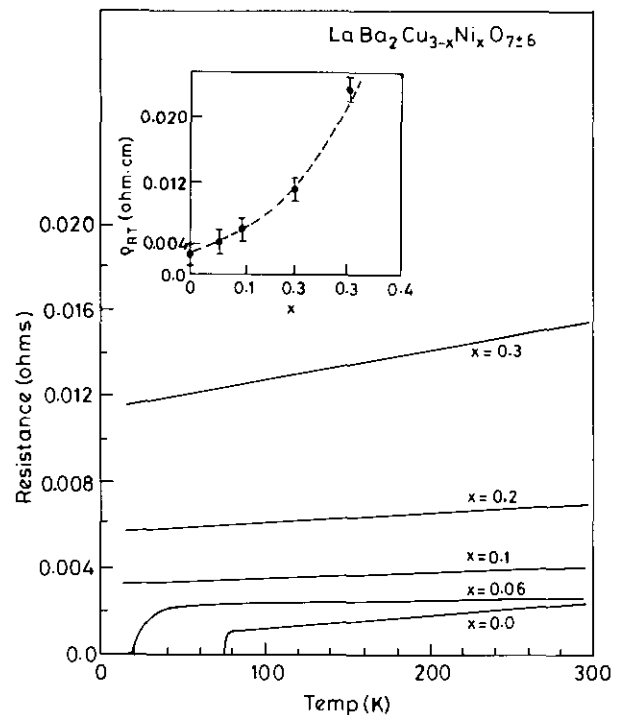


FIG. 7. Temperature variation of resistance of the $\text{LaBa}_2\text{Cu}_{3-x}\text{Ni}_x\text{O}_{7\pm\delta}$. Inset shows the variation of room temperature resistivity as a function of nickel content x .

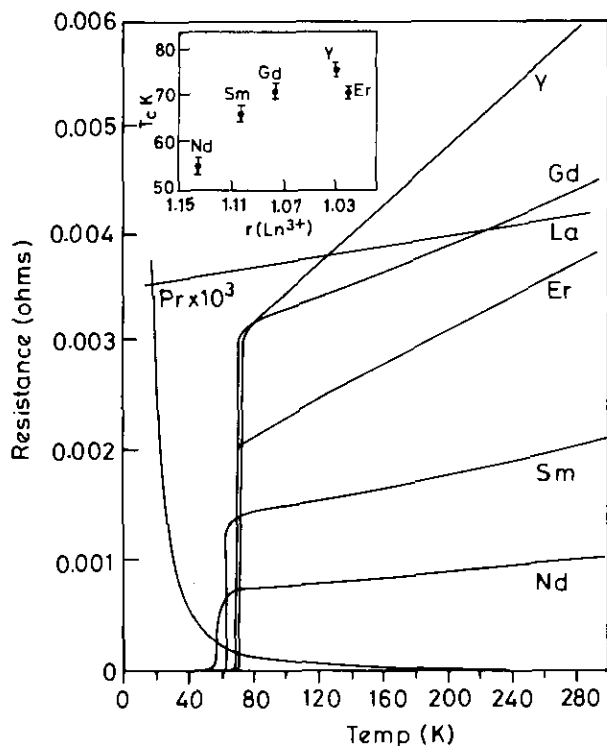


FIG. 8. Temperature variation of resistance of the $\text{LnBa}_2\text{Cu}_{2.9}\text{Ni}_{0.1}\text{O}_{7\pm\delta}$ system of oxides. Inset shows the variation of the superconducting transition temperature T_c as a function of the lanthanide ion radius.

The site preference of nickel could be understood only in terms of the influence of the rare earth ion in controlling the oxygen chemistry and hence the stabilization of the coordination polyhedra (of oxygens) preferred by the 3d transition metal ions in variable valence states. In this connection the control exhibited by the rare earth ion on the diffusivity of oxygen in the $a - b$ basal plane of the 123 system can be accounted for by oxygen mobility, viz. the ease with which oxygen could be reversibly intercalated in the system. So the lanthanum ion with a larger ionic radius is expected to increase the size of the lattice cage and hence enhance free diffusion of oxygen in the basal plane, resulting in the filling up of vacant O(5) sites to ultimately provide the octahedral environment required by a transition metal ion at the Cu(1) site. The enrichment of diffusivity of oxygen in the 123 system by a larger rare earth ion in the place of yttrium has been recently verified by relaxation studies on the longitudinal modes by ultrasonic composite oscillator measurements (23), where lanthanum has been shown to increase the diffusion coefficient (of O_2) by about two orders compared to its yttrium analogue. In the present study, excess oxygen due to Ni substitution is nearly half of the Ni content (see Table 1), indicating an oxidation state of Ni in the 3+ state, analogous to Co substitution for Cu in Y123 (24). Such a

modification of chemical pressure within the cell to stabilize the 123 structure has been observed in the case of the $\text{YSr}_2\text{Cu}_{3-x}\text{M}_x\text{O}_{7+\delta}$ ($M = \text{Co}, \text{Fe}, \text{Ga}, \text{Al}, \text{Mo}, \text{etc.}$) system of oxides, where the substituent ion is known to occupy the Cu(1) site (25–27). The gradual decrease in the peak temperature, and the activation energy for oxygen desorption with increasing nickel content in $\text{LaBa}_2\text{Cu}_{3-x}\text{Ni}_x\text{O}_{7+\delta}$, is consistent with this picture.

The effect of the rare earth ion size on the oxygen diffusivity and hence the directivity on a particular substituent ion to prefer a chain or a sheet site cannot be ascertained without a detailed investigation involving different rare earth ions. So our objective of varying the rare earth ion in $\text{LnBa}_2\text{Cu}_{3-x}\text{Ni}_x\text{O}_{7-\delta}$ ($x = 0.1, 0.2$) was to study the influence of rare earth ions in modifying the chemical pressure in the unit cell. All the $\text{LnBa}_2\text{Cu}_{3-x}\text{Ni}_x\text{O}_{7-\delta}$ series of oxides, except Ni-doped La123, crystallized in orthorhombic structure, analogous to the doping of Ni in Y123. Properties of the $\text{LnBa}_2\text{Cu}_{2.9}\text{Ni}_{0.1}\text{O}_{7\pm\delta}$ system are similar to those of the Ni-substituted Y123 system. T_c of these samples decreased with an increase in the lanthanide ion radius for the same nickel content (see Table 2). This behavior could be attributed to the influence of the rare earth size as observed in the $\text{Ln}_{1-x}\text{Pr}_x\text{Ba}_2\text{Cu}_3\text{O}_{7\pm\delta}$ system of oxides (28, 29).

The non-superconducting, metallic nature exhibited by the higher nickel compositions in La123 are distinctly different, since the transition metal substitutions in the Y123 system studied hitherto showed mostly a gradual transition from a superconducting to semiconducting state without passing through an intermediate metallic state (2). To our knowledge this type of behavior is unique among the analogous systems, which can be attributed to the presence of nickel ions in a 3+ oxidation state in the Cu(1) site.

5. CONCLUSIONS

In conclusion we have shown that

(a) Due to the larger La^{3+} ion size, and an increase in oxygen diffusivity, the $\text{LaBa}_2\text{Cu}_{3-x}\text{Ni}_x\text{O}_{7+\delta}$ system crystallizes in tetragonal structure, where Ni^{3+} ion is suggested to occupy the Cu(1) sites.

(b) The $\text{LaBa}_2\text{Cu}_{3-x}\text{Ni}_x\text{O}_{7+\delta}$ ($0.1 < x < 0.3$) oxides are metallic and non-superconducting down to 4.2 K, which is attributed to the presence of Ni^{3+} ion at the Cu(1) site.

(c) The structural and superconducting properties of the $\text{LnBa}_2\text{Cu}_{3-x}\text{Ni}_x\text{O}_{7+\delta}$ (Ln other than La) system of oxides are analogous to those of nickel-substituted Y123. The superconducting transition temperature decreases with increasing rare earth ion radius. This behavior is suggested to arise from the stabilization of the Ni^{2+} ion at Cu(2) sites.

ACKNOWLEDGMENTS

The authors thank Professor C. N. R. Rao for his encouragement. Discussions with Professor J. Gopalakrishnan have been helpful. The authors also thank Professor S. V. Bhat and Mr. Amit Rastogi for nonresonant microwave absorption measurements. S. R. thanks the University Grants Commission for a Research Fellowship. Financial support for this work from the Department of Science and Technology, Government of India, is gratefully acknowledged.

REFERENCES

1. G. Xiao, M. Z. Cieplak, D. Musser, A. Gavrin, F. H. Streitz, C. L. Chien, J. J. Rhyne, and J. A. Gotaas, *Nature* **332**, 238 (1988).
2. J. M. Tarascon, P. Barboux, P. F. Miceli, L. H. Greene, G. W. Hull, M. Eibschutz, and S. A. Sunshine, *Phys. Rev. B* **37**, 7458 (1988).
3. J. F. Bringley, T. M. Chen, B. A. Averill, K. M. Wong, and S. J. Poon, *Phys. Rev B* **38**, 2432 (1988).
4. R. Sonntag, D. Hohlwein, A. Hoser, W. Prandl, W. Schafer, R. Kiemel, S. Kemmler-Sack, S. Losch, M. Schlichenmaier, and A. W. Hewat, *Physica C* **169**, 141 (1989).
5. T. Kajitani, K. Kusaba, M. Kikuchi, Y. Syono, and M. Hirabayashi, *Jpn. J. Appl. Phys.* **26**, L1727 (1987).
6. T. J. Kistenmacher, *Phys. Rev B* **38**, 8862 (1988).
7. Q. Huang, R. J. Cava, A. Santoro, J. J. Krajewski, and W. F. Peck, *Physica C* **193**, 196 (1992).
8. L. F. Mattheis and D. R. Hamman, *Solid State Commun.* **63**, 395 (1987).
9. P. Zolliker, D. E. Cox, J. M. Tranquada, and G. Shirane, *Phys. Rev. B* **38**, 6575 (1988).
10. T. Siegrist, L. F. Schneemeyer, J. V. Waszczak, N. P. Singh, R. L. Opila, B. Batlogg, L. W. Rupp, and D. W. Murphy, *Phys. Rev B* **36**, 8365 (1987).
11. R. S. Howland, T. H. Geballe, S. S. Laderman, A. Fischer-Colbrie, M. Scott, J. M. Tarascon, and P. Barboux, *Phys. Rev B* **39**, 9017 (1989).
12. P. R. Slater, A. J. Wright, and C. Greaves, *Physica C* **183**, 111 (1991).
13. M. S. Hegde, K. M. Sathyalakshimi, S. Ramesh, N. Y. Vasanthacharya, and J. Gopalakrishnan, *Mater. Res. Bull.* **27**, 1099 (1992).
14. M. S. Hegde, S. Ramesh, and T. S. Panchapagesan, *J. Solid State Chem.* **102**, 306 (1993).
15. D. C. Harris and T. A. Hewston, *J. Solid State Chem.* **69**, 182 (1987).
16. M. S. Hegde, S. Ramesh, and G. S. Ramesh, *Proc. Indian Acad. Sci. (Chem. Sci)* **104**, 591 (1992).
17. S. V. Bhat, P. Ganguly, T. V. Ramakrishnan, and C. N. R. Rao, *J. Phys. C: Solid State Phys.* **20**, L559 (1987).
18. M. H. Ghandehari and S. G. Brass, *J. Mater. Res.* **4**, 1111 (1989).
19. T. Wada, N. Suzuki, A. Maeda, T. Yabe, K. Uchinokura, S. Uchida, and S. Tanaka, *Phys. Rev B* **39**, 9126 (1989).
20. J. M. Tarascon, W. R. McKinnon, L. H. Greene, G. W. Hull, and E. M. Vogel, *Phys. Rev B* **36**, 226 (1987).
21. J. L. Hodeau, C. Chaillout, J. J. Capponi, and M. Marezio, *Solid State Commun.* **64**, 1349 (1987).
22. P. K. Gallagher, H. M. O'Bryan, S. A. Sunshine, and D. W. Murphy, *Mater. Res. Bull.* **22**, 995 (1987).
23. J. L. Tallon and B. E. Mellander, *Science* **258**, 781 (1992).
24. Y. K. Tao, J. S. Swinnea, A. Manthiram, J. S. Kim, J. B. Goodenough, and H. Steinfink, *J. Mater. Res.* **3**, 248 (1988).
25. S. A. Sunshine, L. F. Schneemeyer, T. Siegrist, D. C. Douglass, J. V. Waszczak, R. J. Cava, E. M. Gyorgy, and D. W. Murphy, *Chem. Mater.* **1**, 331 (1991).
26. P. R. Slater and C. Greaves, *Physica C* **180**, 299 (1991).
27. T. Den and T. Kobayasi, *Physica C* **196**, 141 (1992).
28. S. K. Malik, C. V. Tomy, and P. Bhargava, *Phys. Rev. B* **44**, 7042 (1991).
29. Y. Xu and W. Guan, *Physica C* **183**, 105 (1991).